

Rabi oscillations of optical modes in a waveguide with dynamic modulation

Shu-lin Wang¹ · Bing Wang¹ · Cheng-zhi Qin¹ · Kai Wang¹ · Hua Long¹ · Pei-xiang Lu^{1,2}

Received: 15 February 2017 / Accepted: 25 October 2017 / Published online: 4 November 2017
© Springer Science+Business Media, LLC 2017

Abstract We investigate the optical Rabi oscillations in a dual-mode slab waveguide that undergoes a spatial–temporal refractive index modulation. Frequency conversion is induced during Rabi oscillations since dynamic modulation is employed. We also show that the contrast of Rabi oscillations can be controlled by the initial phase of dynamic modulation, which can be tuned arbitrarily from zero to unity as the phase varies. The contrast of zero corresponds to the dynamic supermodes and unity refers to complete Rabi oscillations. It suggests that the phase can be a new degree of freedom to control optical Rabi oscillations. This study may find applications in optical sensors, switches and mode converters.

Keywords Rabi oscillations · Dynamic modulation · Mode conversion

1 Introduction

Rabi oscillation is a very important phenomenon in the two-level system where the atoms exhibit periodic population oscillations under the driving electromagnetic field (Rabi 1936). The Rabi oscillations can be generalized to many other physical systems, such as semiconductors (Schülzgen et al. 1999), atomic and molecular physical systems (Schuh et al. 2009; Tong et al. 2017; He et al. 2017; Yuan et al. 2017; Qin and Zhu 2017; Ma et al. 2017; Hong et al. 2018; Li et al. 2017), and Bose–Einstein condensates (Matthews et al. 1999). Recently, optical analogue of Rabi oscillations have also been demonstrated. The optical Rabi oscillations refer to the periodic mode conversions induced by refractive index modulation. In two-dimensional photonic crystals doped by two coupled single-mode

✉ Bing Wang
wangbing@hust.edu.cn

¹ School of Physics and Wuhan National Laboratory for Optoelectronics, Huazhong University of Science and Technology, Wuhan 430074, China

² Laboratory for Optical Information Technology, Wuhan Institute of Technology, Wuhan 430205, China

cavities, the Rabi oscillations between two cavity modes are reported (Centeno and Felbacq 2000). Also, the Rabi oscillations between two waveguide modes can be induced in the dielectric waveguide with longitudinal index modulation (Kartashov et al. 2007). Moreover, the Rabi oscillations of Floquet–Bloch modes have been realized in waveguide arrays (Makris et al. 2008; Shandarova et al. 2009; Wang et al. 2017a, b, c; Huang et al. 2016; Zhao et al. 2017; Long et al. 2017; Ke et al. 2016; Ke et al. 2017).

In atomic systems, there exists energy transition and frequency shift accompanying the process of Rabi oscillations. However, in the previously demonstrated optical Rabi oscillations, no frequency shift occurs during Rabi oscillations since there only exists spatial modulation of refractive index. To also induce frequency shift to mimic atomic Rabi oscillations, one therefore needs to use dynamic index modulation (Yu and Fan 2009a, b; Fang et al. 2012; Lira et al. 2012; Tzuang et al. 2014; Qin et al. 2016). It also shows that period of Rabi oscillations can be further controlled by varying the dynamic index modulation amplitude.

Apart from controlling the Rabi period, the manipulation of Rabi oscillations contrast is also an important issue. The contrast of Rabi oscillations has been studied in atomic systems (Munz and Marowsky 1986; Schrader et al. 2004; Lupascu et al. 2006; Batalov et al. 2008; Simon et al. 2011). As the frequency of pumped laser is slightly detuned from frequency difference of two atomic levels, the contrast of Rabi oscillations will decrease accordingly. However, the Rabi period will also be shortened. While in optical Rabi oscillations, the control of the contrast hasn't been studied.

In this work, we use dynamic index modulation to realize optical Rabi oscillations and propose a new method to tune the contrast of Rabi oscillations. Without relying on the method of frequency detuning, we utilize the phase of dynamic modulation to control the contrast, which can be tuned arbitrarily from zero to unity. The contrast of zero corresponds to the dynamic supermodes and unity indicates the complete Rabi oscillations. The mechanisms of Rabi oscillations are analyzed from the perspective of mode interferences through the vector superposition methods. The work may find potential applications in optical switches and tunable mode convertors.

2 Optical Rabi oscillations in dynamic waveguide

Firstly, we investigate the concept of Rabi oscillations in dynamic waveguide. Figure 1a is a schematic of waveguide containing a dynamic modulated region. As shown in Fig. 1b, the waveguide supports two transverse electric (TE) polarized modes $|1\rangle$ and $|2\rangle$ at frequencies ω_1 and ω_2 with wave vector k_1 and k_2 , respectively. Photonic interband transitions between $|1\rangle$ and $|2\rangle$ are induced by applying a spatial–temporal permittivity modulation (Yu and Fan 2009a, b),

$$\varepsilon_m(x, z, t) = \delta\varepsilon \cdot \delta(x) \cos(\Omega t + qz + \phi), \quad (1)$$

where $\Omega = \omega_2 - \omega_1$, $q = k_1 - k_2$ are the modulation frequency and wave vector, respectively, which are chosen to satisfy the phase-matching condition, $\delta\varepsilon$ and $\delta(x) = \text{sgn}(x)$ denote the amplitude and transverse distribution of modulation, respectively, and ϕ is the modulation phase which can be set at will. The electric field is expressed as $\mathbf{E}(x, z, t) = \sum_m a_m(z) \mathbf{E}_m(x) \exp[i(\omega_m t - k_m z)]$ with $a_m(z)$ and $\mathbf{E}_m(x)$ ($m = 1, 2$) being normalized complex amplitudes and transverse profiles, respectively (Okamoto 2006). The state spatial evolution equation along the propagation direction is $i\partial_z|\psi\rangle = \mathbf{H}|\psi\rangle$, where

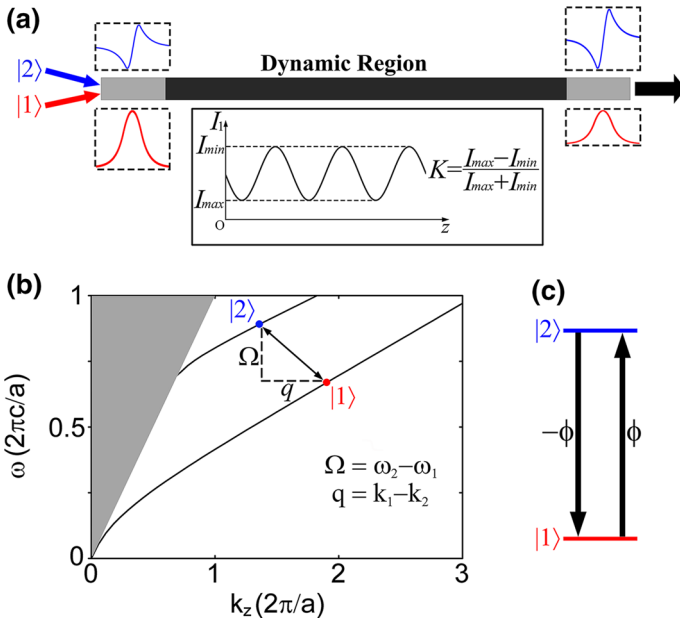


Fig. 1 **a** Schematic of dynamic silicon waveguide with width $d = 0.22 \mu\text{m}$. The black zone represents the dynamic region with length L and permittivity $\epsilon_d + \epsilon_m$ ($\epsilon_d = 12.25$). **b** Band structure of dynamic waveguide. In this essay, the angular frequencies and wavenumbers are normalized with respect to $a = 1 \mu\text{m}$. Red and blue dots denote $|1\rangle$ at lower frequency ω_1 and $|2\rangle$ at higher frequency ω_2 , respectively. **c** Energy levels of dynamic waveguide. (Color figure online)

the superposition state $|\psi\rangle = a_1|1\rangle + a_2|2\rangle$ represents the mixed modes, \mathbf{H} is the state evolution matrix. By substituting the modulation function (1) and the electric field distribution into Maxwell’s equations and using rotating wave approximation (Fang et al. 2012), we obtain

$$\mathbf{H} = \begin{pmatrix} 0 & C e^{-i\phi} \\ C e^{i\phi} & 0 \end{pmatrix}, \tag{2}$$

where $C = \epsilon_0/8 \int_{-\infty}^{+\infty} \delta\epsilon \cdot \text{sgn}(x) E_1(x) E_2(x) dx$ is coupling coefficient between two modes. The amplitude transfer matrix reads

$$\mathbf{T} = \begin{pmatrix} \cos(Cz) & -ie^{-i\phi} \sin(Cz) \\ -ie^{i\phi} \sin(Cz) & \cos(Cz) \end{pmatrix}. \tag{3}$$

Figure 1b shows the band structure of waveguide, where the red and blue dots denote $|1\rangle$ and $|2\rangle$, respectively. Due to the symmetry of modulation function, the dynamic modulation induces both upward photonic transition $|1\rangle \rightarrow |2\rangle$ and downward transition $|2\rangle \rightarrow |1\rangle$, which is analogous to energy level transitions in a two-level atomic system. Here, we regard the waveguide as a two-level system, $|1\rangle$ at lower frequency and $|2\rangle$ at higher frequency are ground state and excited state, respectively. In atomic system, as the laser frequency meets the energy gap between two energy levels, the Rabi oscillations are induced (Rabi 1936). Analogously, as the dynamic modulation satisfies the phase-match condition, the optical Rabi oscillations is realized. Moreover, a photon will carry

modulation phase after transition. In detail, a photon obtain a phase ϕ after upwards transition, while it obtain a phase $-\phi$ after downwards transition (Fig. 1c).

3 Manipulation of the contrast of optical Rabi oscillations

Light wave in $|1\rangle$ and $|2\rangle$ enters the dynamic waveguide with same amplitudes and the phase difference between them is $\Delta\varphi_0$. The incident light wave is expressed as a superposition state $|\psi_0\rangle = \frac{1}{\sqrt{2}}(|1\rangle + e^{i\Delta\varphi_0}|2\rangle)$ (Okamoto 2006). By substituting $|\psi_0\rangle$ into (3), we obtain the intensity of $|1\rangle$ and $|2\rangle$ after normalization,

$$I_1(z) = \frac{1}{2}[1 - \sin(\phi - \Delta\varphi_0) \cdot \sin(2\pi z/L_c)], \tag{4a}$$

$$I_2(z) = \frac{1}{2}[1 + \sin(\phi - \Delta\varphi_0) \cdot \sin(2\pi z/L_c)], \tag{4b}$$

where $L_c = \pi/C$ is the period of Rabi oscillations. Figure 2a shows the intensity spatial evolution of $|1\rangle$ and $|2\rangle$. When $\phi - \Delta\varphi_0$ is $\pi/2$, incident mixed modes can convert to $|1\rangle$ and $|2\rangle$ fully in the modulated zone. As $\phi - \Delta\varphi_0 = 0$, the Rabi oscillations are retained totally. For clarity, the contrast of optical Rabi oscillations is defined as K , where $K = (I_{m,\max} - I_{m,\min}) / (I_{m,\max} + I_{m,\min})$, $I_{m,\max}$ and $I_{m,\min}$ are the maximum and minimum intensity of m th mode ($m = 1, 2$) (Schradler et al. 2004; Lupascu et al. 2006; Batalov et al. 2008; Simon et al. 2011). From Eq. (4), we obtain $K = |\sin(\phi - \Delta\varphi_0)|$. As shown in Fig. 2b, the contrast K reaches maximum when $\phi - \Delta\varphi_0$ is tuned to be $\pm \pi/2$, which corresponds to complete oscillations. With the increase of phase shift on the modulation

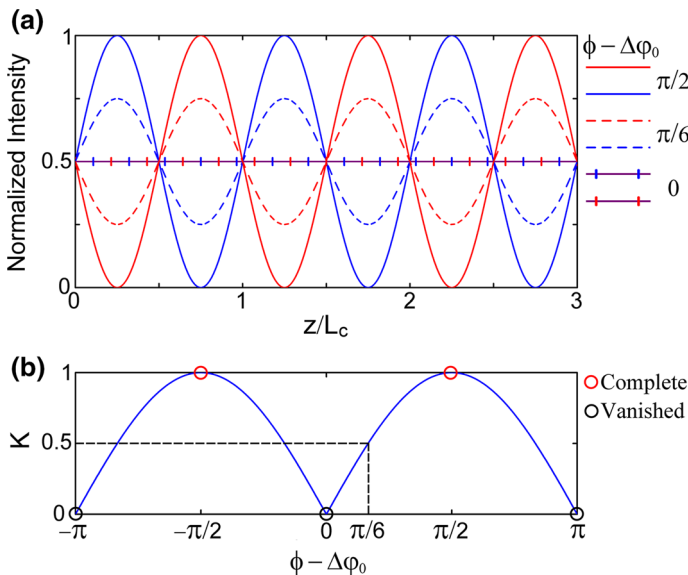


Fig. 2 **a** Intensity spatial evolution of $|1\rangle$ and $|2\rangle$ along with z direction. Red line or line with red marks denote the intensity of $|1\rangle$, the blue ones represents the intensity of $|2\rangle$. **b** The contrast of Rabi oscillations K varying with $\phi - \Delta\varphi_0$. Red and black circles denote complete Rabi oscillations and the situation that Rabi oscillations vanish, respectively. (Color figure online)

phase ϕ , the contrast K is decreasing gradually. At last, no oscillation occurs when $\phi - \Delta\phi_0 = 0$ or $\pm \pi$. Thus, the contrast of optical Rabi oscillations can be controlled by choosing various modulation phases.

Now we focus on the situation that optical Rabi oscillation vanishes, which is associated with dynamic supermodes of waveguide. Under a dynamic modulation with initial phase ϕ , two supermodes $|\psi_+\rangle = \frac{1}{\sqrt{2}}(|1\rangle + e^{i\phi}|2\rangle)$ and $|\psi_-\rangle = \frac{1}{\sqrt{2}}(|1\rangle - e^{i\phi}|2\rangle)$ can be derived from the amplitude transfer matrix (3), where $e^{-i\theta}$ and $e^{i\theta}$ are the corresponding eigenvalues of $|\psi_+\rangle$ and $|\psi_-\rangle$, respectively, where $\theta = Cz$. During propagation, the amplitudes of two modes keep unchanged, the phase difference $\Delta\varphi$ between them remains ϕ or $\phi + \pi$, in other word, $\phi - \Delta\varphi = 0$ or π .

Here, we show the physical mechanism behind the dynamic supermodes by using polar coordinate system. In Fig. 3a–f, the vectors represented by arrows correspond to the modes in waveguide. The length and angle of a vector denote the amplitude and phase of the corresponding mode, respectively. Figure 3a–c show the evolution of supermode $|\psi_+\rangle$, where $\Delta\varphi = \phi$. Amplitudes of incident $|1\rangle$ and $|2\rangle$ are same and the phase difference between them is ϕ , which is shown in Fig. 3a, where red and blue solid arrows denote $|1\rangle$ and $|2\rangle$, respectively. After a distance z , a part of photons initially in $|1\rangle$ is converted to photons in $|2\rangle$ and acquire a phase $-\pi/2 + \phi$, the corresponding amplitude and phase of

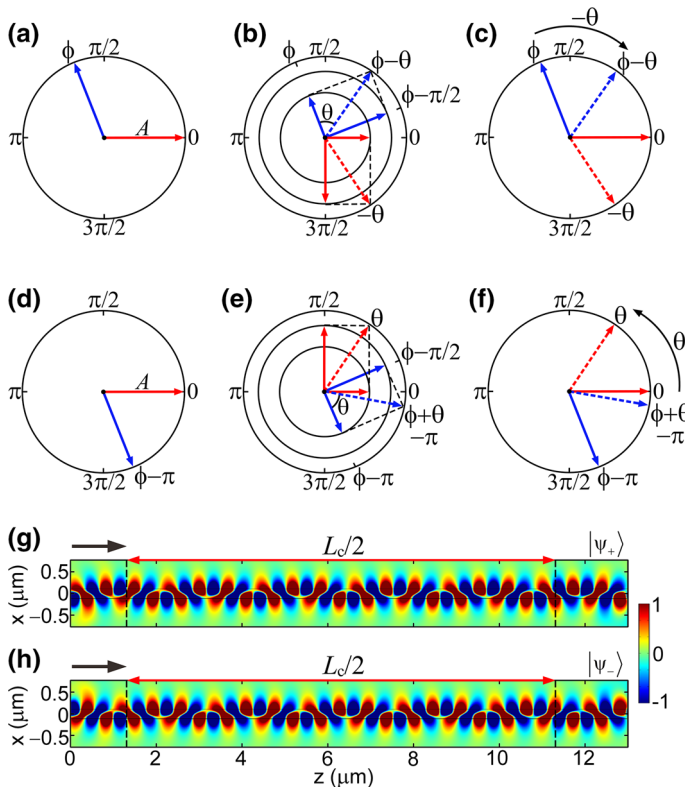


Fig. 3 a–c Evolution of supermode $|\psi_+\rangle$ along with z direction in polar coordinate system. d–f Evolution of supermode $|\psi_-\rangle$ along with z direction in polar coordinate system. Red and blue arrows represent $|1\rangle$ and $|2\rangle$, respectively. g, h Simulated electric field distribution of $|\psi_+\rangle$ or $|\psi_-\rangle$. (Color figure online)

converted $|2\rangle$ are $A\sin\theta$ and $-\pi/2 + \phi$, respectively. The photonic transition is represented by the vector decomposition in polar coordinate system. Similarly, for photons initially in $|2\rangle$, some of them translate into photons in $|1\rangle$ and acquire a phase $-\pi/2 - \phi$, the corresponding amplitude and phase of the converted $|1\rangle$ are $A\sin\theta$ and $-\pi/2$, respectively. The other photons remain unchanged because of experiencing no transition. Now, the interferences both between two $|1\rangle$ modes and between two $|2\rangle$ modes happen. As shown in Fig. 3b, the interference is denoted by the vector superposition, red and blue dashed arrows denote superposed $|1\rangle$ and $|2\rangle$, respectively. The two initial vectors are rotating clockwise in the polar coordinate system while $|\psi_+\rangle$ is propagating in waveguide, and the rotation angle $-\theta$ is proportionate to the propagation distance z . Amplitudes of two modes and the phase difference between them remain unchanged, but two modes get the same phase $-\theta$. Figure 3d–f shows the evolution of eigenstate $|\psi_-\rangle$. The initial phase difference between two modes is $\phi + \pi$. $|1\rangle$ and $|2\rangle$ obtain the same phase θ after propagating over a distance z .

To verify above theoretical analysis, we numerically simulate the field distribution in waveguide by using COMSOL Multiphysics which is based on the finite element method (FEM). Here, the modulation amplitude is chosen as $\delta\epsilon = 0.5$ and the period of Rabi oscillations L_c is $20\ \mu\text{m}$. The frequencies of $|1\rangle$ and $|2\rangle$ are $\omega_1 = 0.6468(2\pi c/a)$ and $\omega_2 = 0.8879(2\pi c/a)$, respectively, the modulation frequency is $\Omega = 0.2411(2\pi c/a)$. The wavenumbers of $|1\rangle$ and $|2\rangle$ are set as $k_1 = 1.8234(2\pi/a)$ and $k_2 = 1.3493(2\pi/a)$, respectively, the wavenumber of dynamic modulation is chosen as $q = 0.4741(2\pi/a)$. As shown in Fig. 3g and h, there exists no mode conversion in the modulated region, which agrees well with the above theoretical analysis.

Thus, the dynamic supermodes are realized as the phase condition $\phi - \Delta\varphi = 0$ or π is satisfied and the amplitudes of two modes are same. To meet above conditions, we could tune the modulation phase ϕ which is determined by the modulator, instead of changing the phase difference $\Delta\varphi$ (therefore $\Delta\varphi$ remain the incident one $\Delta\varphi_0$). Now the contrast of Rabi oscillations becomes 0 and the dynamic waveguide is transparent to the incident mixed modes because of the achievement of supermode.

The mode conversion cancellation induced under specific modulation will make sense in both physics and applications. From the physical perspective, the mode conversion cancellation indicates that Rabi oscillations vanish and the waveguide thus supports two dynamic supermodes. The dynamic supermode here is an optical analogue of the superposition state in a two-level atomic system. Thus we can use the dynamic supermode to simulate the physics of atomic systems with optical settings, such as quantum computing and quantum information processing (Lanyon et al. 2008; O'Brien 2007). From the application point of view, the contrast of Rabi oscillations can be arbitrarily tuned from zero to unity in dynamic modulated waveguide compared to unmodulated one. So it can find applications in optical switches with arbitrary power splitting ratio. And the mode conversion cancellation is only a specific case for the arbitrary power splitting.

After that, we impose a phase shift $\pi/2$ on modulation phase to make $\phi - \Delta\varphi_0$ become $\pi/2$ while supermode $|\psi_+\rangle$ is in process. After propagating over a quarter of Rabi oscillation period, half photons initially in $|1\rangle$ ($|2\rangle$) convert to photons in $|2\rangle$ ($|1\rangle$). After photonic transitions, the amplitudes of two waves in $|1\rangle$ and two waves in $|2\rangle$ are same. For simplification, we only show the phase changes in Fig. 4a. Converted photons in $|2\rangle$ acquire a phase $\phi - \pi/2$, and the phase becomes 0. Converted photons in $|1\rangle$ get a phase $-\phi - \pi/2$, and the phase is $-\pi$. The phase of other photons remain unchanged. The phase difference $\Delta\varphi_2$ between two waves in $|2\rangle$ is 0, thus constructive interference

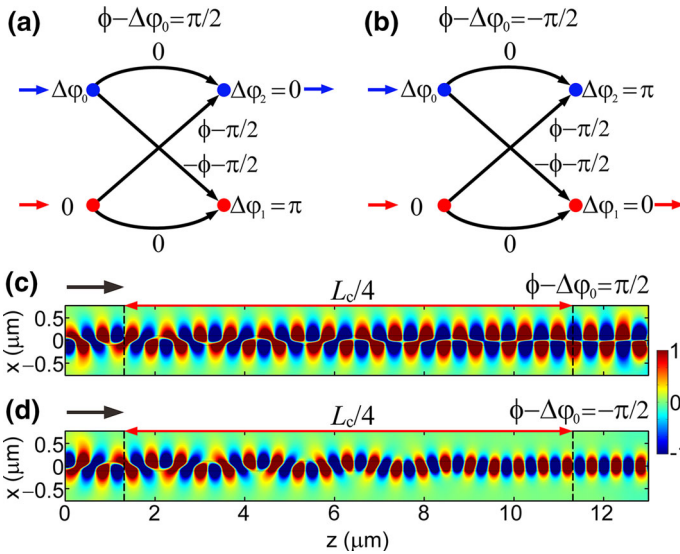


Fig. 4 **a, b** Evolution of mode phase when $\phi - \Delta\varphi_0$ is $\pi/2$ or $-\pi/2$. Red and blue dots represent $|1\rangle$ and $|2\rangle$, respectively. **c, d** Simulated electric field distribution when $\phi - \Delta\varphi_0$ is $\pi/2$ or $-\pi/2$, respectively. (Color figure online)

happens. The phase difference $\Delta\varphi_1$ between two $|1\rangle$ modes is π , thus destructive interference happens and the eventual intensity of $|1\rangle$ becomes 0. Finally, the supermode $|\psi_+\rangle$ converts to $|2\rangle$ completely. The contrast of Rabi oscillations turns from 0 to maximum, in other word, complete Rabi oscillations are realized. For supermode $|\psi_-\rangle$, $\phi - \Delta\varphi_0$ becomes $3\pi/2$ after experiencing the same phase shift $\pi/2$. Here, we only pay attention to one period of ϕ and the range is $-\pi$ to π , thus we replace $3\pi/2$ by $-\pi/2$, actually they have same physical effect on the contrast of Rabi oscillations. As shown in Fig. 4b, supermode $|\psi_-\rangle$ convert to $|1\rangle$ at first and complete Rabi oscillations are also realized.

Figure 4c and d show the simulated electric field distribution when $\phi - \Delta\varphi_0$ is $\pi/2$ and $-\pi/2$, respectively. For supermode $|\psi_+\rangle$, mode profile becomes antisymmetric after going through about $L_c/4$. It means that eigenstate $|\psi_+\rangle$ converts to $|2\rangle$ completely. For supermode $|\psi_-\rangle$, mode profile becomes symmetric. $|\psi_-\rangle$ converts to $|1\rangle$ completely. Therefore, by a phase shift $\pi/2$ on the modulation phase, supermodes are broken and complete Rabi oscillations are induced. If the phase shift is $-\pi/2$, after about $L_c/4$, the consequences are contrary to the above case.

We consider the most general situation in which amplitudes of two incident modes and the phase difference between them are arbitrary, and it is represented as $|\psi_i\rangle = A_1|1\rangle + e^{i\Delta\varphi_0}A_2|2\rangle$, where A_1, A_2 are initial amplitudes of $|1\rangle$ and $|2\rangle$, respectively, and $A_1^2 + A_2^2 = 1$. By substituting $|\psi_i\rangle$ into (3), we obtain the normalized intensity of $|1\rangle$ and $|2\rangle$ along propagation direction,

$$I_1(z) = A_1^2 \cos^2(Cz) + A_2^2 \sin^2(Cz) - A_1A_2 \sin \sin(\phi - \Delta\varphi_0)(2Cz), \tag{5a}$$

$$I_2(z) = A_1^2 \sin^2(Cz) + A_2^2 \cos^2(Cz) + A_1A_2 \sin(\phi - \Delta\varphi_0) \sin(2Cz), \tag{5b}$$

The contrast of Rabi oscillations K reaches minimum $|A_1^2 - A_2^2|$ when $\phi = \Delta\varphi_0$, especially the oscillation vanishes when $A_1 = A_2$. Based on this, the phase difference $\Delta\varphi$ between two modes could be measured. By changing the modulation phase gradually, the modulation is identical to $\Delta\varphi$ until the contrast reaches minimum. As for applications, we could detect the phase shift caused by some perturbations on a sample through the measurement of the changed contrast K . This may have potential applications in the field of optical sensors.

As for experimental proposal, the optical Rabi oscillations could be achieved by both electric modulation and optical modulation. The optical modes for Rabi oscillations are chosen in the optical spectrum, and the index modulation should compensate both the frequency and vector differences between the two modes. Usually, the frequency difference is ~ 10 GHz order of magnitude, which can be implemented by using electro-optical modulation with radiofrequency (RF) signal. Specifically, the dynamic index modulation can be realized by applying the RF voltage through p–n junction diodes on the silicon waveguide (Lira et al. 2012; Tzuan et al. 2014). The modulation wave vector can be introduced by using p–n junction diode arrays with different initial phases. The initial phase of the RF signal in each diode can be continuously tuned by using RF phase shifter.

Due to the limitation of modulation frequency for electro-optic modulation (usually not higher than 40 GHz), the optical pump needs to be employed for higher frequency index modulation. The waveguide is made of light-sensitive material and the dynamic index modulation can be realized through the effect of photoinduced refractive index change. The spatial distribution of index modulation can be controlled by varying the intensity distribution of the illuminated pumped light. The initial phase of the index modulation can be continuously tuned by controlling the arrival time of the pumped light.

4 Conclusion

In summary, we have investigated optical Rabi oscillations in dynamic waveguide. The dual-mode waveguide is regarded as a two-level system and Rabi oscillations are induced by a spatial–temporal refractive index modulation. Due to the introduction of temporal modulation, the frequency shift is realized during mode conversions. The contrast of optical oscillations is studied in this work. We can manipulate the contrast by tuning the initial phase of modulation. Especially, the Dynamic supermodes and complete optical Rabi oscillations are realized. And we analyze the above two cases by using the polar coordinate system and vector superposition. This study may find applications in the optical sensors, switches, mode converters.

Acknowledgements This work was supported by the 973 Program under Grant No. 2014CB921301, the National Natural Science Foundation of China under Grant Nos. 11674117 and 11304108 and the Natural Science Foundation of Hubei Province under Grant No. 2015CFA040.

References

- Batalov, A., Zierl, C., Gaebel, T., Neumann, P., Chan, I.Y., Balasubramanian, G., Hemmer, P.R., Jelezko, F., Wrachtrup, J.: Temporal coherence of photons emitted by single nitrogen-vacancy defect centers in diamond using optical Rabi-oscillations. *Phys. Rev. Lett.* **100**, 077401 (2008)

- Centeno, E., Felbacq, D.: Rabi oscillations in bidimensional photonic crystals. *Phys. Rev. B* **62**, 10101 (2000)
- Fang, K.J., Yu, Z.F., Fan, S.H.: Photonic Aharonov–Bohm effect based on dynamic modulation. *Phys. Rev. Lett.* **108**, 153901 (2012)
- He, M., Zhou, Y., Li, Y., Li, M., Lu, P.: Revealing the target structure information encoded in strong-field photoelectron hologram. *Opt. Quantum Electron.* **49**(6), 232 (2017)
- Hong, Z., Zhang, Q., Rezvani, S. A., Lan, P., Lu, P.: Tunable few-cycle pulses from a dual-chirped optical parametric amplifier pumped by broadband laser. *Opt. Laser Technol.* **98**, 169–177 (2018)
- Huang, H., Ke, S.L., Wang, B., Long, H., Wang, K., Lu, P.X.: Numerical study on plasmonic absorption enhancement by a rippled graphene sheet. *J. Lightw. Technol.* **35**(2), 320–324 (2016)
- Kartashov, Y.V., Vysloukh, V.A., Torner, L.: Resonant mode oscillations in modulated waveguiding structures. *Phys. Rev. Lett.* **99**, 233903 (2007)
- Ke, S.L., Wang, B., Qin, C.Z., Long, H., Wang, K., Lu, P.X.: Exceptional points and asymmetric mode switching in plasmonic waveguides. *J. Lightw. Technol.* **34**(22), 5258–5262 (2016)
- Ke, S.L., Wang, B., Long, H., Wang, K., Lu, P.X.: Topological mode switching in a graphene doublet with exceptional points. *Opt. Quant. Electron.* **49**(6), 224 (2017)
- Lanyon, B.P., Barbieri, M., Almeida, M.P., White, A.G.: Experimental quantum computing without entanglement. *Phys. Rev. Lett.* **101**, 200501 (2008)
- Li, L., Wang, Z., Li, F., Long, H.: Efficient generation of highly elliptically polarized attosecond pulses. *Opt. Quant. Electron.* **49**(2), 73 (2017)
- Lira, H., Yu, Z.F., Fan, S.H., Lipson, M.: Electrically driven nonreciprocity induced by interband photonic transition on a silicon chip. *Phys. Rev. Lett.* **109**, 033901 (2012)
- Long, H., Bao, L., Habeeb, A. A., Lu, P.: Effects of doping concentration on the surface plasmonic resonances and optical nonlinearities in AGZO nano-triangle arrays. *Opt. Quantum Electron.* **49**(11), 345 (2017)
- Lupascu, A., Driessen, E.F.C., Roschier, L., Harmans, C.J.P.M., Mooij, J.E.: High-contrast dispersive readout of a superconducting flux qubit using a nonlinear resonator. *Phys. Rev. Lett.* **96**, 127003 (2006)
- Ma, X., Li, M., Zhou, Y., Lu, P.: Nonsequential double ionization of Xe by mid-infrared laser pulses. *Opt. Quantum Electron.* **49**(4), 170 (2017)
- Makris, K.G., Christodoulides, D.N., Peleg, O., Segev, M., Kip, D.: Optical transitions and Rabi oscillations in waveguide arrays. *Opt. Express* **16**(14), 10309–10314 (2008)
- Matthews, M.R., Anderson, B.P., Haljan, P.C., Hall, D.S., Holland, M.J., Williams, J.E., Wieman, C.E., Cornell, E.A.: Watching a superfluid untwist itself: recurrence of Rabi oscillations in a Bose–Einstein condensate. *Phys. Rev. Lett.* **83**, 3358–3361 (1999)
- Munz, M., Marowsky, G.: Rabi-oscillations without rotating-wave approximation. *Zeitschrift für Physik B Condensed Matter* **63**, 131–137 (1986)
- O’Brien, J.L.: Optical quantum computing. *Science* **318**, 1567–1570 (2007)
- Okamoto, K.: *Fundamentals and Applications of Optical Waveguides*. Elsevier, San Diego (2006)
- Qin, M., Zhu, X.: Molecular orbital imaging for partially aligned molecules. *Opt. Laser Technol.* **87**, 79–86 (2017)
- Qin, C.Z., Wang, B., Long, H., Wang, K., Lu, P.X.: Nonreciprocal phase shift and mode modulation in dynamic graphene waveguides. *J. Lightw. Technol.* **34**(16), 3877–3883 (2016)
- Rabi, I.I.: On the process of space quantization. *Phys. Rev.* **49**, 324–328 (1936)
- Schrader, D., Dotsenko, I., Khudaverdyan, M., Miroshnychenko, Y., Rauschenbeutel, A., Meschede, D.: *Phys. Rev. Lett.* **93**, 150501 (2004)
- Schuh, K., Seebeck, J., Lorke, M., Jahnke, F.: Rabi oscillations in semiconductor quantum dots revisited: influence of LO-phonon collisions. *Appl. Phys. Lett.* **94**, 201108 (2009)
- Schülzgen, A., Binder, R., Donovan, M.E., Lindberg, M., Wundke, K., Gibbs, H.M., Khitrova, G., Peyghambarian, N.: Direct observation of excitonic Rabi oscillations in semiconductors. *Phys. Rev. Lett.* **82**, 2346 (1999)
- Shandarova, K., Rüter, C.E., Kip, D., Makris, K.G., Christodoulides, D.N., Peleg, O., Segev, M.: Experimental observation of Rabi oscillations in photonic lattices. *Phys. Rev. Lett.* **102**, 123905 (2009)
- Simon, C.M., Belhadj, T., Chatel, B., Amand, T., Renucci, P., Lemaître, A., Krebs, O., Dalgarno, P.A., Warburton, R.J., Marie, X., Urbaszek, B.: Robust quantum dot exciton generation via adiabatic passage with frequency-swept optical pulses. *Phys. Rev. Lett.* **106**, 166801 (2011)
- Tong, A.H., Zhou, Y.M., Lu, P.X.: Bifurcation of ion momentum distributions in sequential double ionization by elliptically polarized laser pulses. *Opt. Quantum Electron.* **49**(2), 77 (2017)
- Tzuan, L.D., Fang, K.J., Nussenzeig, P., Fan, S.H., Lipson, M.: Non-reciprocal phase shift induced by an effective magnetic flux for light. *Nat. Photonics* **8**, 701–705 (2014)

- Wang, Z.Q., Wang, B., Long, H., Wang, K., Lu, P.X.: Surface plasmonic lattice solitons in semi-infinite graphene sheet arrays. *J. Lightw. Technol.* **35**(14), 2960 (2017a)
- Wang, Z.Q., Wang, B., Long, H., Wang, K., Lu, P.X.: Surface vector plasmonic lattice solitons in semi-infinite graphene-pair arrays. *Opt. Express* **25**(17), 20708–20717 (2017b)
- Wang, F., Qin, C.Z., Wang, B., Ke, S.L., Long, H., Wang, K., Lu, P.X.: Rabi oscillations of plasmonic supermodes in graphene multilayer arrays. *IEEE J. Quantum Electron.* **23**(1), 4600105 (2017c)
- Yu, Z.F., Fan, S.H.: Complete optical isolation created by indirect interband photonic transitions. *Nat. Photonics* **3**, 91 (2009a)
- Yu, Z.F., Fan, S.H.: Optical isolation based on nonreciprocal phase shift induced by interband photonic transitions. *Appl. Phys. Lett.* **94**, 171116 (2009b)
- Yuan, H., Li, F., Long, H.: Control of high-order harmonic generation with chirped inhomogeneous fields. *JOSA B* **34**(11), 2390–2395 (2017)
- Zhao, D., Wang, Z. Q., Long, H., Wang, K., Wang, B., Lu, P. X.: Optical bistability in defective photonic multilayers doped by graphene. *Opt. Quantum Electron.* **49**(4), 163 (2017)